Influence of Wear Volume on Surface Quality in Grinding Process Based on Wear Prediction Model

Wei Cao
Zhao Han (hanzhao1996@163.com)
Xi'an Technological University https://orcid.org/0000-0003-3233-848X
Ziqi Chen
Zili Jin
Jiajun Wu
Jinxiu Qu
Dong Wang

Research Article

Keywords: grinding, surface quality, wear model, wear volume, grinding temperature, surface morphology

Posted Date: December 13th, 2021

DOI: https://doi.org/10.21203/rs.3.rs-1148125/v1

Influence of wear volume on surface quality in grinding process based on wear prediction model

Cao Wei [1], Han Zhao [1], Chen Ziqi [1], Jin Zili [1], Wu Jiajun [1],Qu Jinxiu [1], Wang Dong [2]
[1].School of Mechatronic Engineering, Xi'an Technological University，Xi'an Shaanxi 710021, China；
[2]. Shaanxi Province Institute of Water Resources and Electric Power Investigation and Design，Xi'an Shaanxi 710001，China;

Corresponding author:
Han Zhao, Xi'an Technological University，2 Xuefu Road, Xi'an Shaanxi 710021, China；
Email: hanzhao1996@163.com

Abstract

In the grinding process, the workpiece would not only be cut by abrasive grains, but also have adhesive wear caused by high temperature and heavy load, which makes the surface quality of the workpiece worse. In this paper, a wear test method considering speed, force, wear coefficient, temperature and hardness was proposed. A new wear prediction physical model was established based on finite element method and numerical simulation technology. The wear test was carried out on a grinding machine. The comprehensive research on the relationship between force, temperature, surface morphology and wear volume of grinding process was studied. The relationship between workpiece speed, grinding depth, cooling lubrication conditions and wear volume of grinding process was studied. The results show that the wear model can achieve numerical prediction and trend prediction of grinding temperature, surface profile and wear volume, the relative errors between the theoretical and actual values of wear and grinding temperature are 9.84% and 2.07% respectively. This study provides a support for wear prediction and surface quality control of grinding process from the perspective of temperature and micro material removal form.

Key words: grinding; surface quality; wear model; wear volume; grinding temperature; surface morphology

V	mm^3	Wear volume
s	μm	Relative sliding distance
K	-	Wear coefficient of one dimension
H	HV	Hardness of the worn surface
W	N	Normal contact force
h	μm	Wear depth
p	Pa	Contact pressure
D_{gx}	μm	Abrasive diameter
D_{mean}	μm	Average diameter of abrasive grains
σ	-	Standard deviation
F_n	N	The normal grinding force
α	°	Cutting angle
F_b	N	Brinell hardness test force
d	μm	Indentation diameter
μ	-	Friction coefficient
a_e	μm	Grinding depth
s_p	μm^2	The longitudinal projection area of contact area between the abrasive and the workpiece
k	-	Wear coefficient
q_t	℃	Heat flux in contact area
v_s	m/s	Speed of grinding wheel
v_w	m/s	Speed of workpiece
l_g	μm	The contact arc length
b	μm	The contact width
Q		structure number
v_g	-	Abrasive ratio (Proportion of abrasive volume to total volume)
N	-	The number of abrasive grains in the contact area
λ	W/(m·c)	Coefficient of thermal conductivity
ρ	Kg/m^3	density
C	J/(kg·c)	The specific heat capacity
ε_w		The proportion of heat transferred to the workpiece
i	-	The number of analysis steps
X	μm	The distance between each point

V	mm^3	Wear volume
L	μm	The measured length of workpiece
S_m	mm^2	Units wear area

Research highlights:

1. Proposed a wear prediction physical model considering speed, contact force, temperature, wear coefficient and material hardness for grinding process, which can predict surface morphology.
2. A method for measuring and calculating surface wear in grinding process was proposed.
3. The grinding temperature field, wear volume, surface morphology and wear mechanism are analyzed, which provides technical support for improving grinding surface quality from the perspective of grinding burn and grinding.

Influence of wear volume on surface quality in grinding process based on wear prediction model

Abstract

In the grinding process, the workpiece would not only be cut by abrasive grains, but also have adhesive wear caused by high temperature and heavy load, which makes the surface quality of the workpiece worse. In this paper, a wear test method considering speed, force, wear coefficient, temperature and hardness was proposed. A new wear prediction physical model was established based on finite element method and numerical simulation technology. The wear test was carried out on a grinding machine. The comprehensive research on the relationship between force, temperature, surface morphology and wear volume of grinding process was studied. The relationship between workpiece speed, grinding depth, cooling lubrication conditions and wear volume of grinding process was studied. The results show that the wear model can achieve numerical prediction and trend prediction of grinding temperature, surface profile and wear volume, the relative errors between the theoretical and actual values of wear and grinding temperature are 9.84% and 2.07% respectively. This study

provides a support for wear prediction and surface quality control of grinding process from the perspective of temperature and micro material removal form.

Key words: grinding; surface quality; wear model; wear volume; grinding temperature; surface morphology

1. Introduction

With the rapid development of industrialization, grinding is used widely in aviation manufacturing and other fields, but its high temperature, speed, heavy load working conditions will cause severe wear on the surface of the workpiece, and reducing the surface quality. The research of wear prediction model and wear mechanism can predict the wear volume and trend, so as to provide support for controlling the surface quality of workpieces ,and reduce the cost of grinding quality test.. Therefore, this research has a great significance. However, the factors affecting wear volume are various, including temperature, speed, force, wear coefficient, hardness and so on. For this reason, scholars have done a lot of research on the wear volume.

Anirban naskar [1] studied the wear mechanism of electroplated CBN grinding wheel in different grinding fluid cooling and lubrication conditions and its influence on grinding performance, which contributed to the improvement of grinding wheel dressing and grinding quality. Mehmet Fatih Kahraman [2] designed a grinding wheel with C-shaped groove and used it in the test. According to the test data, the linear regression equation that can predict the roughness was obtained, combined with Monte Carlo simulation technology, the measurement uncertainty of surface roughness was predicted. This method can predict the surface roughness of the grinding wheel under various grinding conditions in advance. Gokhan Aydin [3] studied the wear performance of diamond saw blade cutting rock, developed a saw blade wear measurement method based on optical imaging principle, and used this method to compare the influence and contribution of various processing parameters and wear amount SWR, which proved the accuracy of SWR prediction model. Tianyu Yu [4] proposed a novel phenomenological model for the progressive wheel wear to study the failure behavior of the grinding wheel at high temperature. The results show that high efficiency deep grinding (HEDG) configuration can deliver much higher material removal for the same amount of wheel wear. Chenwei Dai [5] defines abrasive wear as four types: crescent depression on the rake face, abrasion on the

flank face, grain micro-fracture, and grain macro-fracture, and discussed the influence of abrasive wear on material removal behavior. The results show that the material removal efficiency is proportional to the wear width on the grain rake face. Li Benkai [6] studied the evolution of concave wear behavior and its effect on material removal under different un-deformed chip thickness and grinding wheel speed， which provide a technical support for monitoring the grain wear during grinding.

At present, scholars have done a lot of research on the wear evolution in the grinding process, but most of the research is oriented to the surface failure mechanism of grinding wheel. Although a few scholars have studied the material removal behavior caused by single grinding wheel abrasive grain wear, they have not studied the material removal mechanism from the perspective of material wear.

Sieniawski [7] studied the effect of different machining parameters on the grinding force of steel CrVI2. Li [8] established a grinding temperature model for free-form surface workpiece, and verified the model by test. However, he uses thermocouple to collect temperature data, which requires the workpiece to be cut into two parts, and it has an impact on the test results. Curtis [9] analyzed the temperature field, residual stress and morphology in grinding process, but did not study the interaction mechanism between them. Li [10] established a material removal model for double-sided grinding, which can predict the grinding profile of the workpiece surface, and analyzed the material removal uniformity according to its calculation results, but obviously did not consider the influence of temperature on the material removal mechanism. Qu [11] established a new workpiece surface roughness prediction model according to the young's modulus formula, improved the grinding thickness index according to the energy balance assumption, and reduced the prediction deviation from 63.9% to 13.9%, but a large part of the grinding energy is converted into heat energy, which should also be considered.

The above research provided the basis for the research of grinding from the temperature, force and material removal mechanism, but there is no comprehensive research on the relationship between temperature, force, surface morphology, r and wear.

Hsu [12] made statistics on the factors affecting the wear amount; the results show that 30 factors have been considered in the past. Zhang [13] studied the relationship between friction dissipation power and wear rate, but did not consider the change of lubrication conditions. Ma [14] proposed an elastohydro dynamic

lubrication model, and the wear amount was studied from three aspects of temperature, pressure and speed by the integrative test bench of axis piston pump. However, he did not study the response of different lubricating medium to wear. Ramalho [15] used the Archard wear model to study the relationship between contact pressure, speed and wheel-rail wear. But at present, the maximum running speed of the train has reached more than 600 km/h, the contact temperature between wheel and rail is also affected by the speed, therefore, if this model can be linked with temperature and improved, it can provide more support for train maintenance.

Above scholars have studied the relationship between varies factors and wear amount, however, if a wear prediction model considering all the above factors can be established, the accuracy of prediction would be improved substantially.

Reference		1	2	3	4	5	6	7	8	9	10	11	12	13	14	15	This paper
Grinding wear	Single grinding wheel abrasive grain wear					√	√										√
	Grinding wheel wear	√	√	√	√		√	√	√	√							√
	Material removal	√			√	√			√		√	√	√				√
Wear model	Force	√	√		√	√	√						√	√	√	√	√
	Temperature				√								√		√		√
	Speed	√	√	√	√	√	√						√	√	√	√	√
	Cooling lubrication conditions	√		√									√				√
Study on grinding	Grinding force	√	√		√	√	√	√	√		√	√	√				√
	Grinding temperature	√							√				√				√
	Wear amount			√	√	√	√	√		√							√
	Surface morphology		√	√			√				√	√					√
	Material removal mechanism	√	√	√	√	√					√	√					√

Fig. 1 Summary of references and research contents

The previous research has achieved satisfactory results, their respective research contents are summarized as shown in Fig. 1, but there are still some defects and knowledge gaps: (Ⅰ)The proposed wear model and wear mechanism are not suitable for grinding process. (Ⅱ) Lack of a wear prediction model and a wear test method that comprehensively considers speed, force, temperature, wear coefficient and hardness. (Ⅲ) There is no comprehensive research on the relationship between temperature, force, surface morphology and wear of grinding process.

In this paper, a wear test method of grinding process was proposed，which can change the workpiece speed, grinding depth, cooling lubrication conditions at the

same time, consider the effects of speed, contact force, temperature, wear coefficient and hardness on the wear volume. A new prediction model of wear and surface topography of grinding process was established by using finite element method and numerical simulation technology. The influence of different processing parameters on the wear volume was analyzed, and the wear mechanism of grinding process based on temperature field, wear volume and surface morphology was studied, which provides a support for controlling the surface quality of workpiece.

2. Wear failure mode of grinding process

Grinding is widely used in ultra-precision machining of thin-wall parts; the small cutting feeds of abrasive grains on the surface of grinding wheel (abrasive wear) makes it have higher machining accuracy than cutting. However, the working conditions of high temperature, high speed and heavy load cause adhesive wear of the surface material, which would affect the surface quality of grinding.

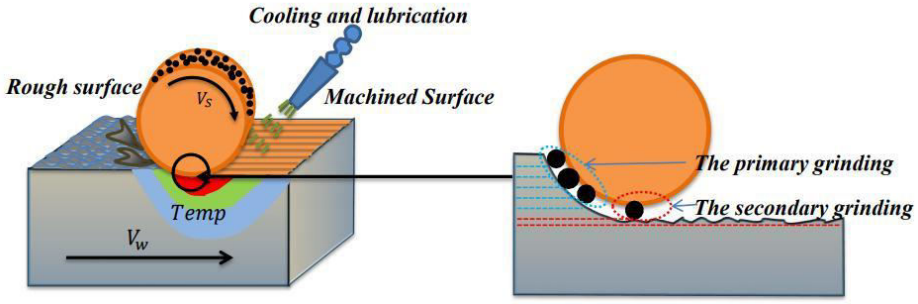

Fig. 2 Schematic diagram of grinding material removal

Binhua Gao and Wenxi Wang [16-17] divide the grinding process into two periods: primary grinding and secondary grinding, as shown in Fig. 2. The primary grinding is abrasive wear caused by the single abrasive cutting material, and the material removal volume caused by it is determined as the cutting depth layer of abrasive, which is defined as macro material removal; the secondary grinding is adhesive wear caused by high temperature and pressure at the bottom of the contact area between abrasive and workpiece, which is defined as micro material removal. Therefore, the total volume of material removal is the sum of the two stages.

Although the material removal volume of secondary grinding is small, it plays a decisive role in grinding surface quality. Therefore, this paper focuses on the material removal mechanism, wear volume and surface quality control of secondary grinding.

The grinding machine can control the processing parameters, including

workpiece speed, grinding depth and cooling lubrication conditions, these parameters would affect the relative speed, temperature, grinding force, wear coefficient and material properties, so its wear process is complex. Due to the different diameter of the abrasive grains on the surface of the grinding wheel, the contact force of each single abrasive grain in the contact area is also different, which leads to the change of the contact pressure and wear depth per unit area. Therefore, in this paper, the contact area between the grinding wheel and the workpiece was discretized to study the wear volume caused by the single abrasive, which can not only calculate the overall wear volume, but also study the wear mechanism.

3. Establishment and Calculation of wear prediction model

3.1 Basic calculation model of wear volume

In 1953, J.F. Archard of the United States put forward the Archard adhesive wear theory, which holds that when the surface of the friction pair slides relatively, the adhesive point shears and breaks due to the adhesive effect, resulting in a lot of micro volume falling off on the material [18]. Based on the Archard wear model, the wear model of grinding process was established

$$\frac{V}{s} = K\frac{W}{H} \tag{1}$$

where V is the wear volume, s is the relative sliding distance, K is the wear coefficient of one dimension, H is the hardness of the worn surface, and W is the normal contact load.

The size of the abrasive grains on the grinding wheel would cause the change of contact force, so each contact point on the contact surface was discretized:

$$\frac{dh}{ds} = \frac{K}{H}p \tag{2}$$

where h is the wear depth, p is the contact pressure. The integral form of EQ. 2 is

$$h = \int_0^s \frac{K}{H} pds = \int_0^s kpds \tag{3}$$

3.2 Contact pressure

It is assumed that the abrasive grains are spherical. Hou [19] made statistics on the diameter of abrasive grains of the grinding wheel, the results show that the

diameter of abrasive grains obeys normal distribution, and the probability function is

$$P\left(D_{gx}\right)=\frac{1}{\sigma\sqrt{2\pi}}\exp\left[-\frac{1}{2}\left(\frac{D_{gx}-D_{mean}}{\sigma}\right)^{2}\right] \tag{4}$$

where D_{gx} is the abrasive diameter, D_{mean} is the average diameter of abrasive grains, σ is the standard deviation.

In this paper, the grinding wheel with granularity of 46 was selected for test, the grain diameter ranges from 38 μm to 45 μm, which would affect the normal contact force. When the move direction of single abrasive grain is horizontal relative to the surface of the workpiece, it is in the ploughing stage, which also indicates that the grinding depth is in the maximum, as shown in Fig. 3. Because of the abrasive grains in the ploughing stage is very similar to the Brinell hardness test indicator, and the white corundum abrasive grains can be regarded as a rigid body by the characteristic of high hardness, therefore, the contact force can be deduced according to the principle of Brinell hardness measurement [20].

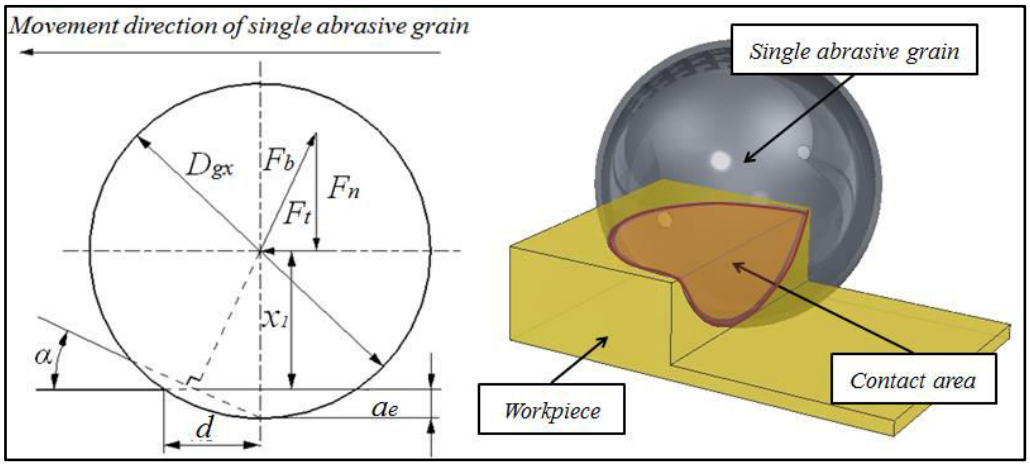

Fig. 3 Ploughing stage of single grain

$$H=\frac{2F_{b}}{\pi D_{gx}\left(D_{gx}-\sqrt{D_{gx}{}^{2}-d^{2}}\right)} \tag{5}$$

The normal grinding force F_n can be obtained by cutting angle α

$$\alpha=\arccos\left(1-\frac{2a_{e}}{D_{\mathrm{gx}}}\right) \tag{6}$$

$$F_{n}=F_{\mathrm{b}}(\cos\alpha-\mu\sin\alpha) \tag{7}$$

where F_b is Brinell hardness test force, d is indentation diameter, μ is the friction

coefficient, a_e is grinding depth.

As shown in Fig. 3, the red area represents the contact area between the abrasive and the workpiece, and its longitudinal projection area is S_p. In this paper, the contact pressure per unit area model of a single abrasive grain was established, and the abrasive diameter is normally distributed, the contact pressure p between the grinding wheel and the workpiece was discretized.

$$S_p = \frac{1}{2}\pi\left[(\frac{D_{gx}}{2})^2 - (D_{gx} - a_e)^2\right] \tag{8}$$

$$p = \frac{F_n}{S_p} \tag{9}$$

3.3 Grinding temperature

Some scholars assumed that the wear coefficient k is not affected by temperature, which is feasible at low temperature, but severe wear is always accompanied by high temperature, such as grinding, it may reach above 700℃, which would bring error in wear prediction. Therefore, the calculation of temperature field is necessary.

The work done by the grinding wheel to grind the workpiece is converted into the heat flow [21], and the grinding process is performed by all single abrasive grains; therefore, the premise of calculating the force is to get the number of abrasive grains. In this work, a new heat model was established based on the granularity (grain size) and structure number Q (abrasive ratio) of grinding wheel

$$q_t = \frac{\mu F_n N(v_s + v_w)\times 10^{12}}{l_g b} \tag{10}$$

where, v_s is the speed of grinding wheel, v_w is the speed of workpiece, l_g is the contact arc length, b is the contact width.

It is assumed that the abrasive grains are evenly distributed on the surface of the grinding wheel, as shown in Fig. 4. Then, the average clearance of abrasive grains can be calculated by the abrasive ratio V_g (Proportion of abrasive volume to total volume) of the grinding wheel, and the number of abrasive grains N in the contact area can be obtained.

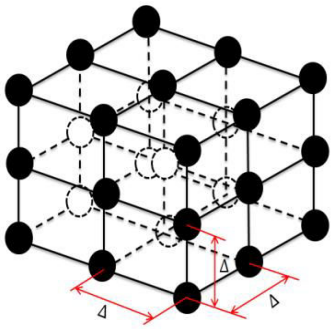

Fig. 4 Distribution of abrasive grains on the surface of the grinding wheel

$$V_g = \frac{62 - 2Q}{100} \tag{11}$$

$$\Delta = \sqrt[3]{\frac{\pi D_{mean}{}^3}{6V_g}} \tag{12}$$

$$N = \frac{l_g b}{\Delta^2} \tag{13}$$

The heat flux generated by grinding would be transmitted to the workpiece and grinding wheel in a certain proportion [22], which is determined by the material properties.

$$\varepsilon_w = \left[1 + \sqrt{\frac{(\lambda\rho c)_s v_s}{(\lambda\rho c)_w v_w}}\right]^{-1} \tag{14}$$

$$q_w = \varepsilon_w q_t \tag{15}$$

where λ is the coefficient of thermal conductivity, ρ is the density, c is the specific heat capacity, ε_w is the proportion of heat transferred to the workpiece.

Finite element method can solve the heat conduction. Firstly, the model was established and the material properties were imported. Then, reduce the mesh size of the surface layer of the workpiece, as shown in Fig. 5(a). The heat flux and heat transfer coefficient were added to each contact surface, and its moving direction is the same as the direction of relative movement. According to the relative speed, the analytical field calculation formula of each analysis step was deduced and established, as shown in EQ. 16. Finally, the model was calculated, and the result is shown in Fig. 5. It can be seen that the temperature tends to be stable in the tenth analysis step, and the stable temperature was used as the statistical index.

In this work, GH4169 nickel-base superalloy was used for grinding test, GH4169

nickel-base superalloy, and white corundum abrasive and grinding fluid are shown in Tab. 1 and Tab. 2.

$$C_{input_i} = \frac{2}{l_g} X_i - \frac{l_g}{7} i \tag{16}$$

where, i is the number of analysis steps, and X is the distance between each point where the load was applied and the end of the workpiece.

Tab. 1 Material properties of GH4169 [23]

θ / ℃	11	100	200	300	400	500	600	700	1000
k/[W/(m×K)]	13.4	14.7	15.7	17.8	18.3	19.6	21.2	22.8	30.4
$c/(J/(kg \cdot C))$	-	-	-	481.4	493.9	514.8	539.0	573.4	707.4

Tab. 2 Thermal properties of the grinding fluid and white corundum abrasive grains

Tab. 2 Grinding fluid material parameters

Material Science	Water-based grinding fluid	Oil-base grinding fluid	White corundum abrasive
Initial viscosity μ_0/(Pa× s)	0.00415	0.0415	
Density ρ/(kg/m^3)	1000	830	3960
Coefficient of thermal conductivity k/[W/(m×K)]	0.68	0.15	28.82
Specific heat capacity c/[J/(kg× K)]	4180	2000	765

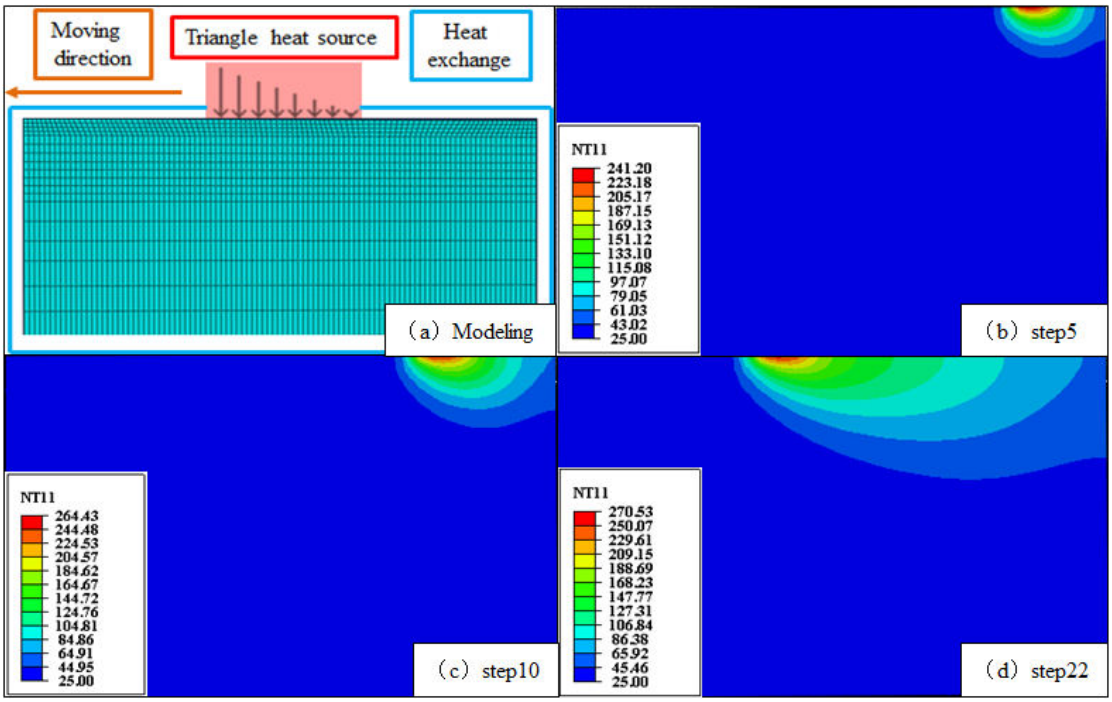

Fig. 5 Modeling and results of grinding temperature

3.4 Wear coefficient *K*, material hardness *H* and relative sliding distance *s*

Lee [24] improved the Archard wear model, and obtained the relationship between temperature and hardness *H*. Rabinowicz [25] has tested and summarized the wear coefficient *K* under different lubrication conditions, as shown in the Tab. 3. The content of aluminum oxide in white corundum abrasive grains is more than 99%, so the contact between white corundum and GH4169 is metal-nonmetal. In addition, oil-based grinding fluid has good lubrication performance, and water-based grinding fluid also contains about 50% emulsion. Therefore, according to the table below, the wear coefficient *K* of dry grinding, water-based grinding fluid and oil-based grinding fluid are assumed to be 1.7×10^{-6}, 1.65×10^{-7} and 3.3×10^{-7}, respectively.

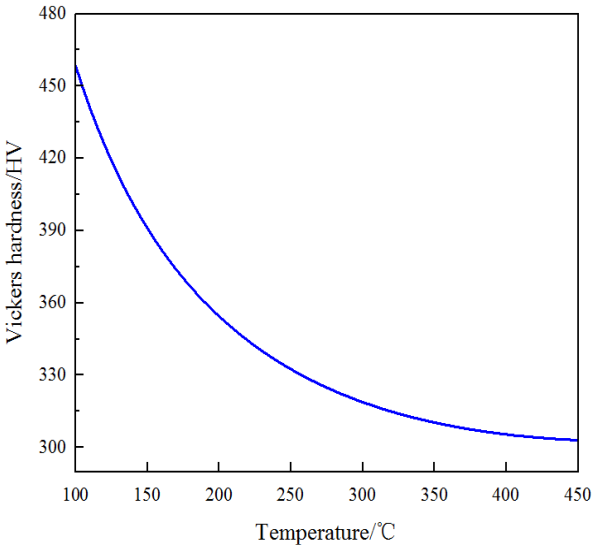

Fig. 6 Hardness for GH4169

Tab. 3 Wear coefficient tested by Rabinowicz [24]

Lubrication condition	Metal–metal		Nonmetal–metal
	Similar	Dissimilar	
Clean surface	1.7×10^{-3}	6.7×10^{-5}	1.7×10^{-6}
Poor lubrication	6.7×10^{-5}	3.3×10^{-5}	1.7×10^{-6}
General lubrication	3.3×10^{-6}	3.3×10^{-6}	1.7×10^{-6}
Good lubrication	3.3×10^{-7}	3.3×10^{-7}	3.3×10^{-7}

The unit sliding distance s of abrasive grain at the contact point can be calculated by integrating the relative sliding speed. Due to the down grinding method (The rotation direction of the grinding wheel is opposite to the direction of movement of the worktable) was adopted in the test; the sliding distance can be calculated as follows:

$$s = \int_{t_i}^{t_{i+1}} v dt = \int_{t_i}^{t_{i+1}} v_s + v_w dt \tag{17}$$

3.5 Calculation results and discussion

The program was designed according to the model established in the previous chapter and applicable to the wear prediction of any grinding wheel for grinding metal materials; its flow is shown in the Fig. 7:

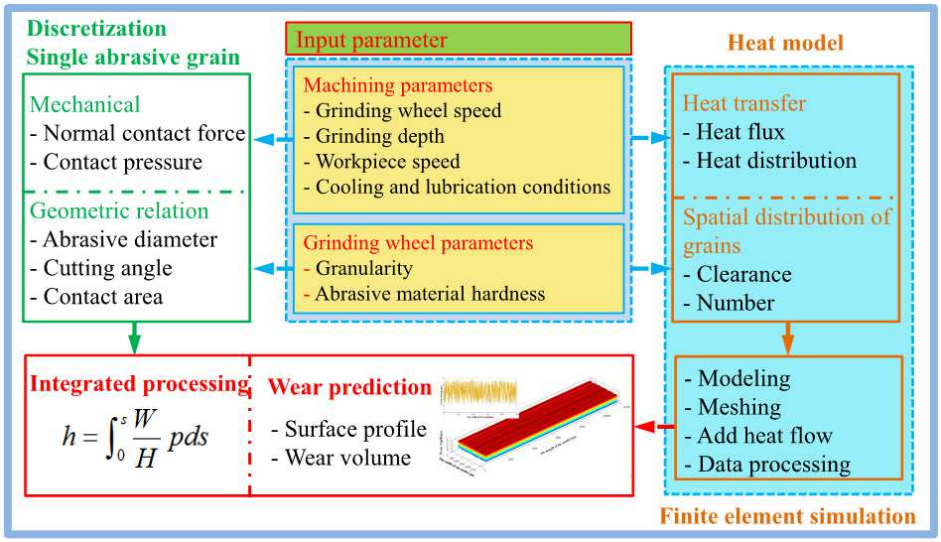

Fig. 7 Wear prediction steps

(1)Firstly, input the machining parameters (grinding wheel speed, grinding depth, workpiece speed and cooling and lubrication conditions) and grinding wheel parameters (granularity and abrasive material hardness).

(2)According to the input parameters, the geometric characteristics between abrasive grains and materials are obtained, and the contact force and contact pressure are calculated.

(3)At the same time, the heat flux distribution ratio and heat flux density of grinding temperature field are obtained according to the input parameters, and the temperature field is obtained by finite element method.

(4)The results of contact force model and temperature model are input into Archard wear model, and assuming that the wear depth along the length direction of the workpiece is the same, the surface profile and wear volume of the workpiece can be obtained.

Calculation results	Import the processing parameters
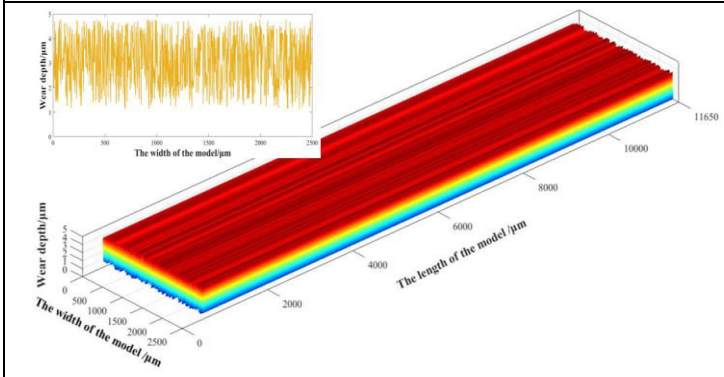	a_e=0.02mm
	v_w=0.18m/s
	Dry grinding
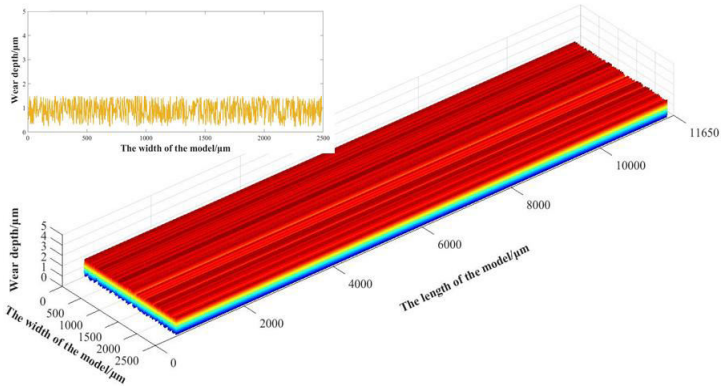	a_e=0.02mm
	v_w=0.18m/s
	Water-base Grinding Fluid
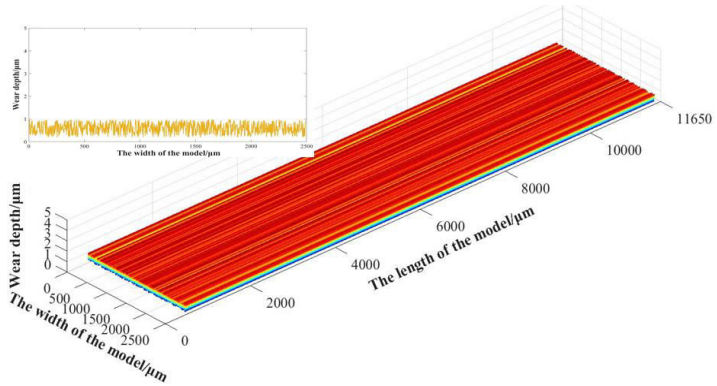	a_e=0.02mm
	v_w=0.18m/s
	Oil-base Grinding Fluid

Fig. 8 Solution results of wear model (surface profile)

The simulation results show that the grinding fluid can reduce the wear, and the smaller the wear volume is, the greater the surface profile fluctuation is.

4. Grinding and wear test results and discussion

4.1 Test rig

27 workpieces made of GH4169 nickel-base superalloy with the size of "30mm × 20mm × 15mm" were tested. ELB plane grinder was used for datum surface processing. MYH3070 hydraulic transmission grinder was selected for test, the

spindle speed is 1450rpm, and its grinding wheel speed is 15m / s. The abrasive grains of the grinding wheel are made of white corundum, the granularity is 181, the structure number is 5, and the diameter is 200 mm. The testo868 infrared thermal imager manufactured by Testo was used to collect the thermal images, its measurement range is -25℃~650℃, accuracy is ± 2℃. The zegage plus white light interferometer produced by Zygo was used to measure the surface topography. In this test, three different cooling lubrication conditions were adopted, including dry grinding, water-based grinding fluid and oil-based grinding fluid. Two kinds of grinding fluid are used in the ratio of 5%.

4.2 Test condition

ELB plane grinder has high machining accuracy, its grinding depth is only 2μm at most, but the abrasive diameter range is 38~45μm, which makes the comparison of results under different processing parameters not obvious. Before the test, all workpieces need to have the same precision datum plane. Therefore, in this test, all workpieces were super finished by ELB plane grinder, and then tested by MYH3070 hydraulic drive grinder, which can not only ensure that the workpieces have the same datum plane, but also obtains obvious results comparison. Change the grinding wheel speed, grinding depth and grinding fluid during the experiment, aiming the lens of the infrared thermal imager with the grinding contact area and record the data in time, and then imported it into the post-processing software for in-depth analysis. After the experiment, place the workpieces under the white light interferometer to measure the surface profile and morphology.

The test bench and scheme are as follows. According to the process parameters, a three factor three level full factor test was designed.

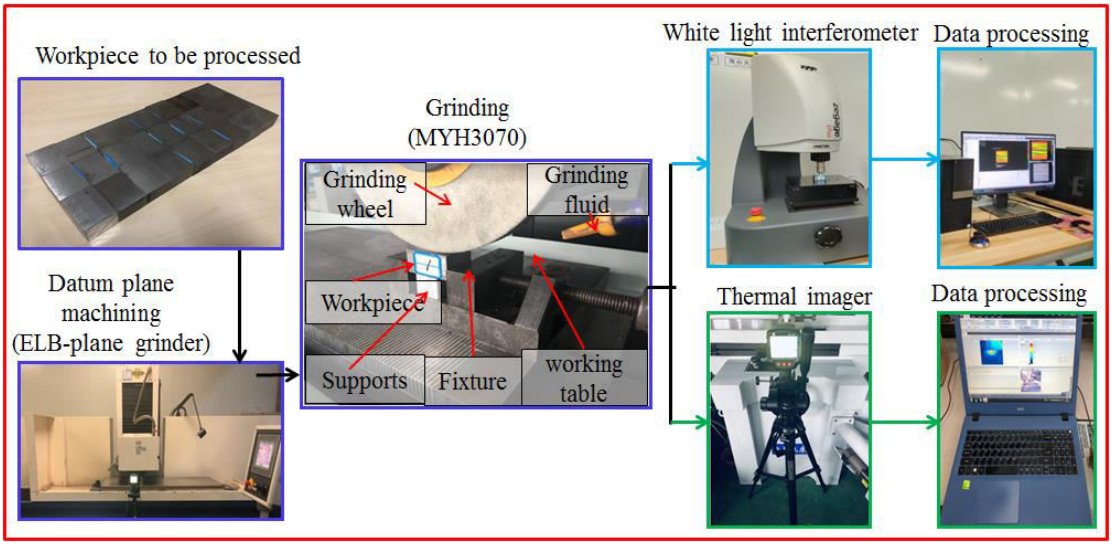

Fig. 9 Test rig and schemes

Tab .4 Factors and level of the test

Level / Factor	1	2	3
Grinding depth (mm)	0.02	0.04	0.06
Speed of workpiece (m/s)	0.18	0.24	0.3
Cooling Lubrication Conditions	Dry grinding	Water-base grinding Fluid	Oil-base grinding Fluid

4.3 Testing techniques of grinding temperature and its data processing

Aiming the lens of the infrared thermal imager with the grinding contact area and record the data in time, and then imported it into the post-processing software for in-depth analysis and recording the hot spot (maximum temperature) [26].

Compared it with FEM results, it can be seen from Fig. 10(a) that there is a heat distribution relationship between the grinding wheel and the workpiece, and the heat flux transferred into the workpiece is greater than that of the grinding wheel, this infrared measurement result is better than that obtained by other scholars using thermocouples. The simulated temperature nephogram is similar to the thermal imaging nephogram; the above results proved that the finite element analysis results are consistent with the measured results.

4.4 Testing techniques of Surface topography and its data processing

Place the processed workpieces under the white light interferometer to scan the surface profile，because the white light interferometer collects the surface profile

slowly and has a large number of specimens, a rectangular area of 2.5mm × 11.65mm was selected in the middle of the upper surface of the workpieces for sampling. In addition, four contour lines in the width direction of the workpieces were selected in the rectangular area for measurement, and the average value was taken as the final contour line. Fig. 10(b) listed some of the measurement results and sampling methods of the profile, and the white light interferometer can measure the surface profile and surface morphology at the same time. The numerical simulation results are similar to the surface profile sampling results, which proved the accuracy of the wear prediction model.

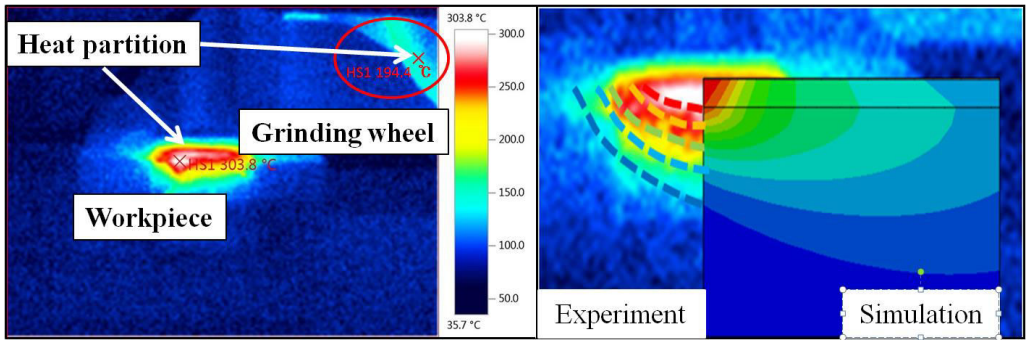

(a) Infrared thermography of grinding temperature

Processing parameters of the experiment	Surface morphology	Wear profile in width direction
ae=0.02mm *vw*=0.18m/s Dry grinding	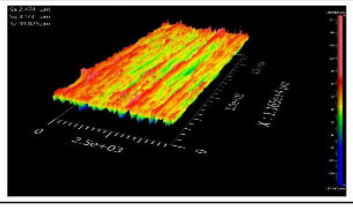	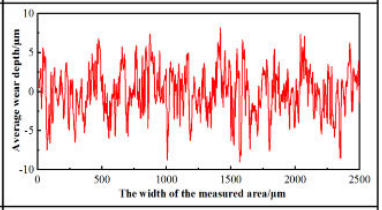
ae=0.02mm *vw*=0.18m/s Water-base Grinding Fluid	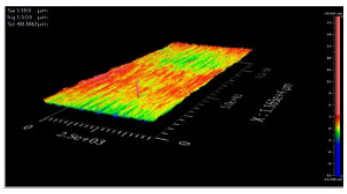	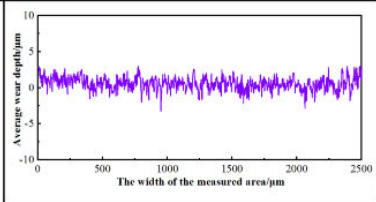
ae=0.02mm *vw*=0.18m/s Oil-base Grinding Fluid	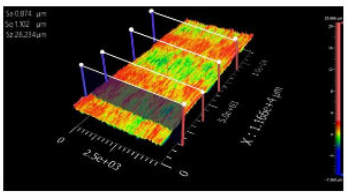	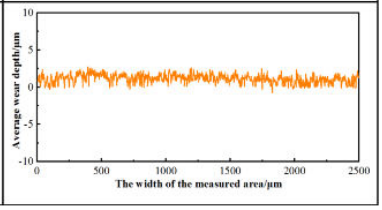

(b) Acquisition results of the surface graphology(dry grinding, water-based, oil-based)

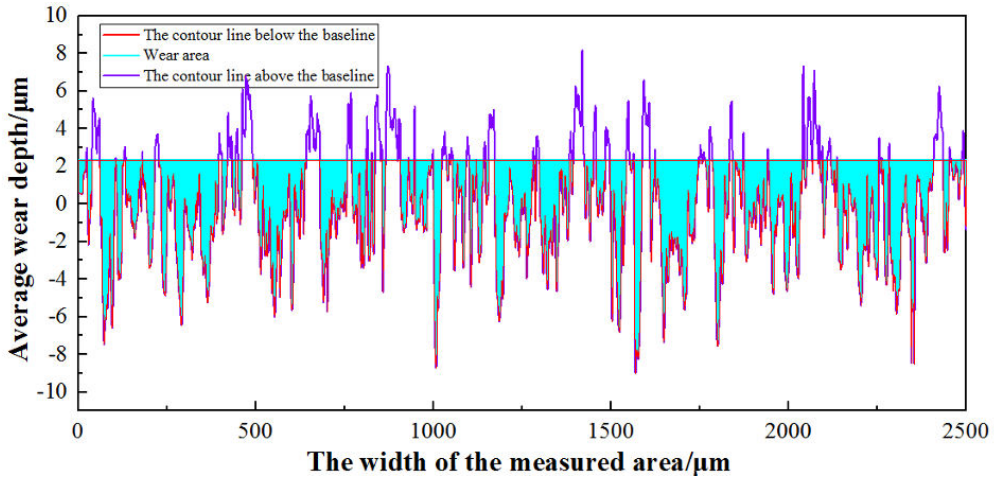

(c) Wear profile along the width of workpiece

Fig. 10 Test results and data processing

Due to the normal distribution of abrasive size, the contact pressure and wear depth of each contact point are different, resulting in irregular surface profile of workpiece after grinding. Therefore, in this paper, the contour arithmetic mean deviation of the average contour was selected as the baseline height. Then, the units wear area S was obtained by calculating the area enclosed by the baseline and the contour line below the baseline, which is shown as the blue area in Fig. 10(c), the calculation method is shown in EQ. 18 and 19. Finally, the wear volume V was obtained. 27 groups of data were processed according to the above steps.

$$y = \frac{1}{6000}\sum_{i=1}^{6000}|y_i| \tag{18}$$

$$V = S_m \cdot L = L \cdot \int_0^{2500}(y - y_i)dx \tag{19}$$

where L is the measured length of workpiece and S_m is the units wear area.

5. Discussion

By comparing and analyzing the wear volume and surface quality, and taking the grinding temperature field and surface roughness as evidence, the wear mechanism of grinding workpiece surface under various machining parameters was studied.

5.1 Relationship between grinding depth and wear volume

The water-based grinding fluid was selected as the cooling and lubricating medium, the wear volume of each grinding depth under different workpiece speeds is

shown in Fig. 11(a). The wear volume increases with the increase of grinding depth, and the trend of the measurement results is consistent with the simulation results.

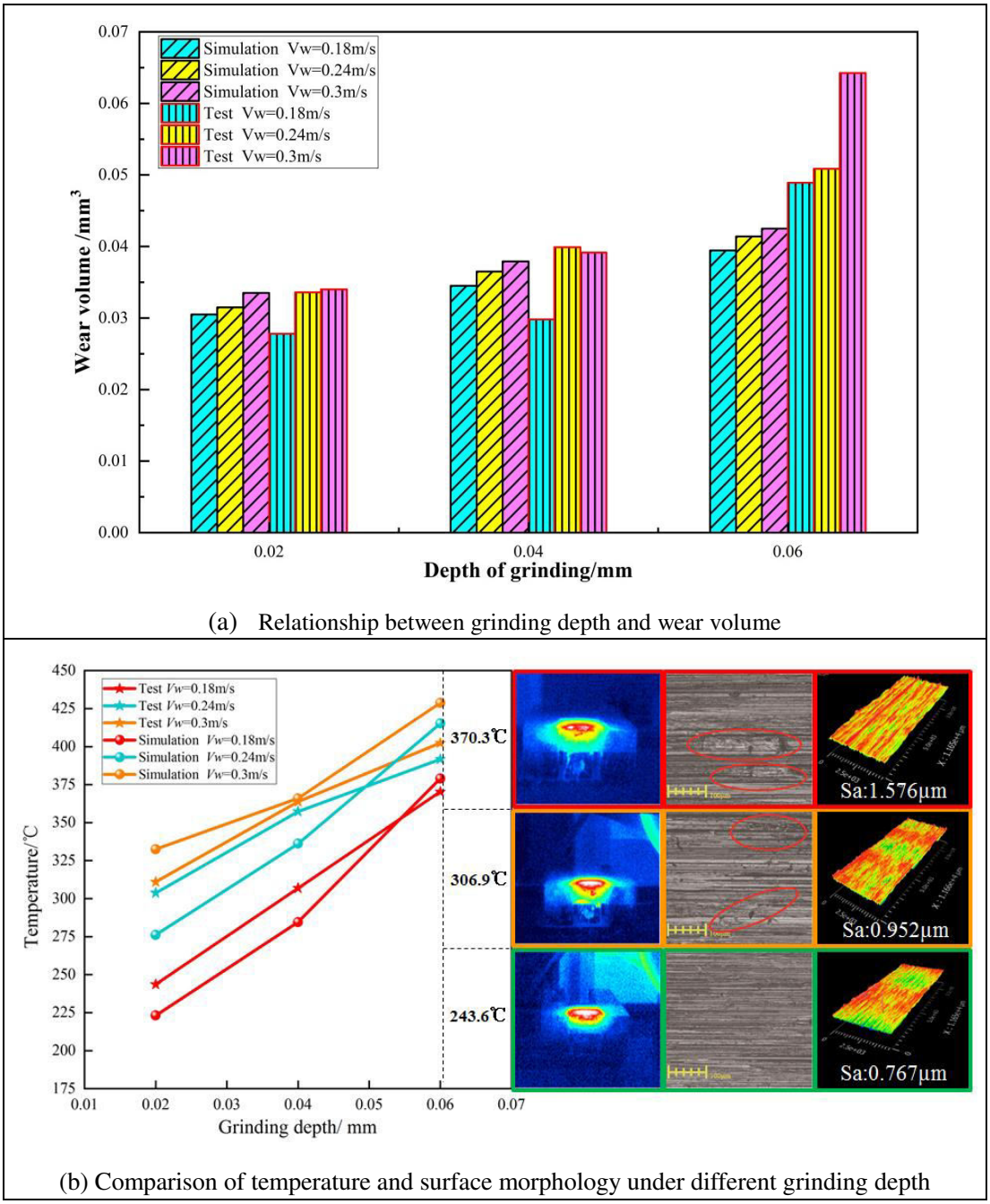

(a) Relationship between grinding depth and wear volume

(b) Comparison of temperature and surface morphology under different grinding depth

Fig. 11 Comparison of test data under different grinding depth

After studied the mechanism, it was found that: the increase of the longitudinal grinding depth of the grinding wheel would lead to the increase of cutting depth of single abrasive, and the envelope surface formed by the workpiece and white corundum abrasive in the ploughing stage will increase. Resulting in the increase of the contact force of abrasive grains, so that the contact pressure per unit area increases

and accelerate the wear of the workpiece; In addition, with the increase of abrasive contact pressure, more heat will be generated in the contact area, resulting in an increase in the temperature of the contact pair and a drop in the hardness of the material, so that the wear more severe than before.

From the above analysis, it can be seen that temperature has a crucial influence on the wear volume. Therefore, the temperature field, wear volume, surface morphology and surface roughness of grinding process were compared and analyzed. It is found that the smaller the wear volume, the smaller the workpiece roughness and the smoother the surface, which is the same as the theoretical simulation results.

When the temperature reaches 240 ℃(a_e=0.02mm), the ploughing scratch of single abrasive grain is very clear and there is no burn mark; when the temperature reaches 300 ℃(a_e=0.04mm), the material near the scratch begin to soften and become fuzzy due to high temperature, part of the material is pulled down due to adhesive wear (marked in the red area in the Fig. 11(b)); when the temperature reaches 370 ℃ (a_e=0.06mm), the high temperature causes the material soften severely, the extrusion of the abrasive grains on the material makes these materials stick together, and the traction force when the grinding wheel separates from the workpiece causes the material to fall off, forming pits on the surface of the workpiece. In addition, high temperature would cause residual stress on the surface of the workpiece, resulting in cracks.

The results show that there is a positive correlation between grinding depth and wear volume. Therefore, in the actual working conditions, on the premise of ensuring the working efficiency, the longitudinal grinding depth should be reduced, so as to avoid the material softening, adhesive wear and cracks caused by high temperature.

5.2 Relationship between workpiece speed and wear volume

When the longitudinal grinding depth of the grinding wheel was kept at 0.02mm, the wear volume of each workpiece speed under different cooling lubrication conditions is shown in the Fig. 12. When the moving speed of the worktable is increases from 0.18m/s to 0.3m/s, the wear volume increases slowly.

The mechanism was analyzed as follows: as the moving speed of the worktable

increases, the relative speed of the single abrasive and the workpiece increases, the time taken to remove the same volume of material decreases, the heat generated per unit time increases, and the hardness of the material decreases.

Because of the relative velocity does not change much, the temperature and wear volume change little.

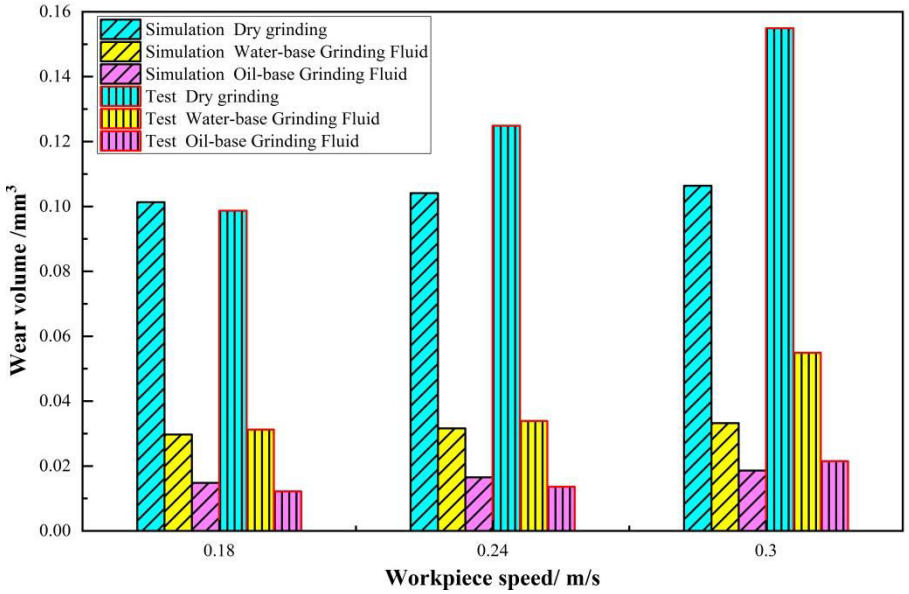

Fig. 12 Influence of grinding depth speed on wear

5.3 Relationship between cooling lubrication conditions and wear volume

When the horizontal moving speed of the worktable was kept at 0.24m/s, the wear volume of each cooling lubrication conditions under different grinding depths is shown in Fig. 13(a). The results show that the wear volume is the most severe under dry grinding condition, and the water-based grinding fluid and oil-based grinding fluid can reduce the wear volume by 72.77% and 88.15%, respectively. The relative error of the results is calculated according to the above data

$$\delta_T = \frac{\overline{T_m} - \overline{T_p}}{\overline{T_p}} \qquad \delta_Q = \frac{\overline{V_m} - \overline{V_p}}{\overline{V_p}}$$

where T represents the temperature, V represents the wear volume, δ means the relative error, and the subscripts m and p represent the measured value and the theoretical predicted value respectively.

After calculation, the relative errors between the theoretical and actual values of wear and grinding temperature are 6.14% and 2.07% respectively, which is more

accurate than the prediction model of A.Ramalho's，and verified the accuracy and effectiveness of the algorithm.

The reason for this is that in the case of dry grinding, the contact area can only dissipate heat by convection heat transfer with air under dry grinding condition; on the contrary, the convective heat transfer performance of the grinding fluid make grinding fluid able to take away a large amount of heat energy. In addition, the debris generated by grinding accumulate in the contact area and easily stick to the workpiece under dry grinding condition, and a small part of them is embedded in the abrasive clearance, but the grinding fluid can wash away the debris in time, reduce the temperature and wear volume of the workpiece.

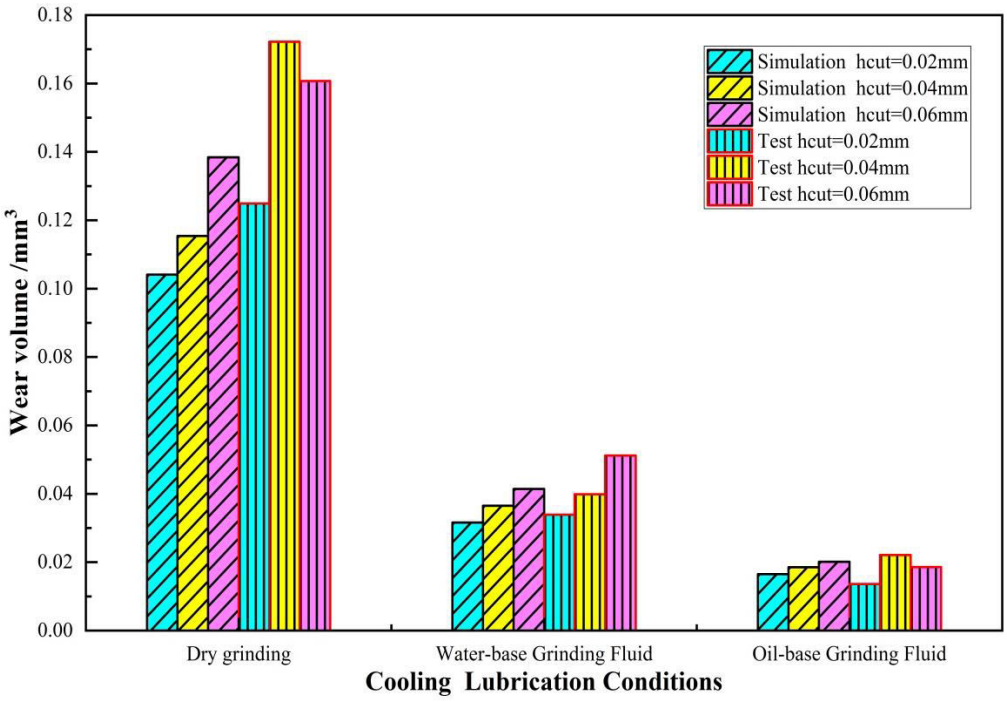

(a) Relationship between cooling lubrication conditions and wear volume

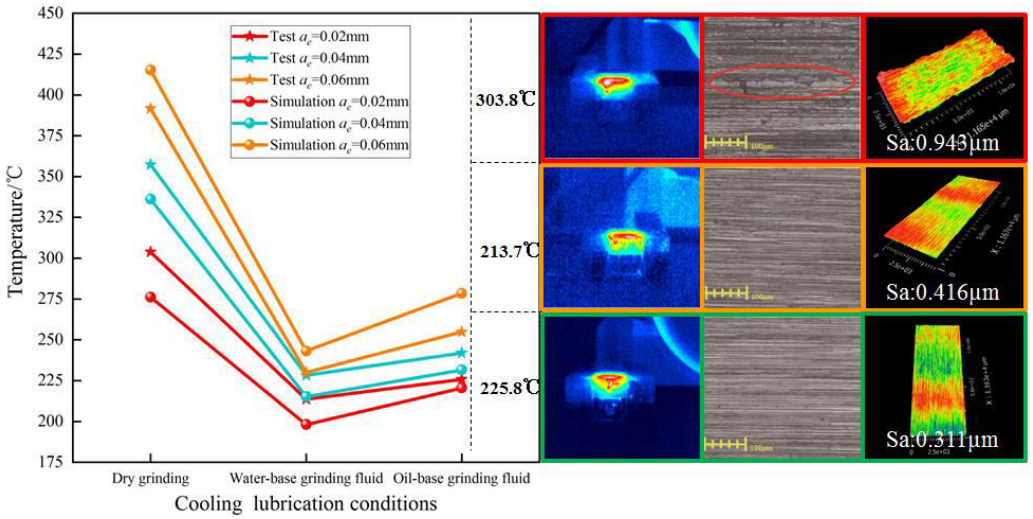

(b) Comparison of temperature and morphology under different cooling lubrication conditions

Fig. 13 Comparison of test data under different cooling lubrication conditions

It can be seen from Fig. 13 that the surface quality and roughness becomes worse with the increase of the wear volume, and the wear volume is closely related to the grinding temperature. Compared with the dry grinding condition, water-based grinding fluid and oil-based grinding fluid reduce the temperature by 29.66% and 25.67%, respectively, which indicated that the cooling performance of water-based grinding fluid is better than that of oil-based grinding fluid, but the difference was not significant.

Grinding fluid can reduce wear volume by about 80%. The anti-wear property of oil-based grinding fluid is better than that of water-based grinding fluid, this is because the oil-based grinding fluid easy to form lubrication film and reduce friction, the wear coefficient can be reduced several times in the contact area between metal and non-metal.

In conclusion, the influence of lubrication performance (reduce wear coefficient) on wear volume is greater than that of cooling performance (reduce material hardness). Before actual machining, if the grinding temperature is predicted to be higher than 300 ℃, oil-based grinding fluid can be used for cooling and lubrication; Otherwise, use water-based grinding fluid to focus on cooling, which can improve the surface quality of the workpiece according to the actual situation.

5.4 Study on wear morphology

Fig. 14 shows the surface morphology of workpiece under different cooling lubrication conditions after grinding, and their wear volume are 0.022mm^3, 0.039mm^3 and 0.172mm^3, respectively.

As can be seen from Fig. 14 (a), there are many scratches (white box selected area), which are abrasive wear caused by the single abrasive on the workpiece. In addition, due to the adhesive wear between the grinding wheel and the workpiece, some scratches disappear due to the material falling off. However, the oil-based grinding fluid can cool and lubricate the workpiece in time, which reduces the material removal and makes the surface smoother than before. As shown in the morphology, the wear area and depth are small The surface is smooth and flat to form a mirror effect.

The lubrication performance of water-based grinding fluid is worse than that of oil-based grinding fluid. As shown in Fig 14(b), there are many black spots on the surface, the color is darker than that of oil-based grinding fluid, and the wear range and depth increase. this is because the viscosity of water-based grinding fluid is lower than that of oil-based grinding fluid, so it has worse protection ability to the surface of the workpiece.

The morphology of the workpiece under dry grinding condition is as shown in Fig. 14(c), the wear depth is increased, and the range of material falling off area becomes larger than before, some debris are accumulated on the surface and not removed. This is because the high temperature reduces the hardness of the material and makes the material stick together, and finally it is removed in block form. In addition, without grinding fluid, the debris on the surface of the workpiece cannot be washed away in time, so there is still some grinding debris left on the surface.

Therefore, in order to ensure the grinding surface quality, smaller cutting depth and workpiece speed should be selected(a_e = 0.02mm, v_w = 0.18m / s), and oil-based grinding fluid should be selected for cooling and lubrication.

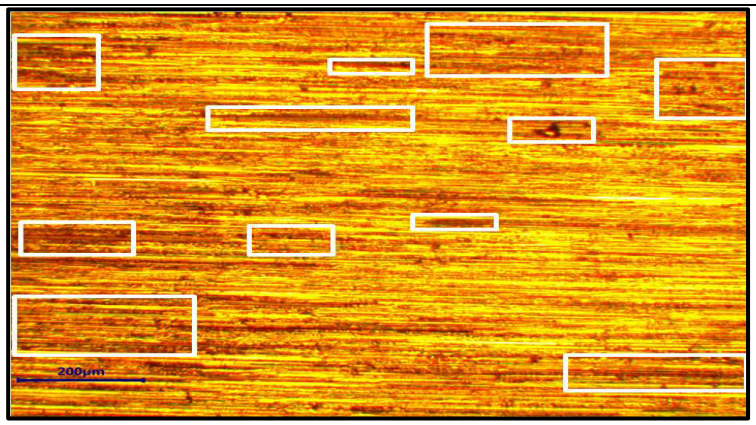

(a) Oil based grinding fluid (wear volume = 0.022mm^3)

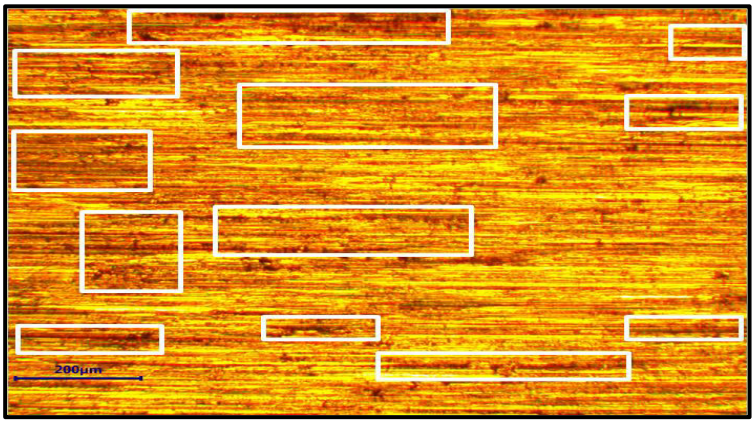

(b) Water based grinding fluid (wear volume =0.039mm^3)

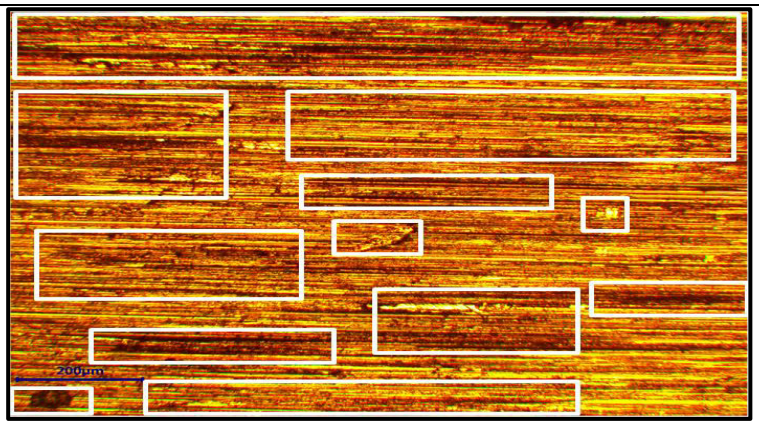

(c) Dry grinding (wear volume = 0.172mm^3)

Fig. 14 Morphology under different cooling lubrication conditions

6. Conclusion

Based on the finite element method and numerical simulation technology, the physical model of wear prediction of grinding process was established, and the wear profile, grinding temperature and wear volume in grinding process are obtained, the results show that the relative error between the theoretical value and the actual value of wear is 6.14%, which provides support for the prediction of workpieces surface

morphology in grinding process under different process parameters. In addition, an improved grinding heat model was established, and the comprehensive research on the relationship between temperature, force, surface morphology and wear under different working conditions was studied.

A method for measuring and calculating the wear volume of grinding process was proposed. The experimental results and simulation results were compared and analyzed, and provide a reference for the control of surface quality in the actual grinding process from the perspective of processing parameters.

The wear mechanism of grinding process was studied, and the temperature field, wear volume and surface morphology were compared and analyzed, which provides optimal machining parameters for improving the surface quality from the perspective of grinding burn and adhesive wear (ae = 0.02mm, vw = 0.18m / s and oil-based grinding fluid).

In the future, the wear deviation caused by machine tool vibration will be considered.

References

[1] Naskar A, Choudhary A, Paul S (2020) Wear mechanism in high-speed superabrasive grinding of titanium alloy and its effect on surface integrity - sciencedirect. Wear, 462–463. https://doi.org/10.1016/j.wear.2020.203475

[2] Mehmet Fatih Kahraman, Sabri Öztürk (2019) Experimental study of newly structural design grinding wheel considering response surface optimization and Monte Carlo simulation. Measurement, 147(C), pp. 106825-106825.
https://doi.org/10.1016/j.measurement.2019.07.053

[3] Aydin G, Karakurt I, Aydiner K (2013) Wear Performance of Saw Blades in Processing of Granitic Rocks and Development of Models for Wear Estimation. Rock Mechanics and Rock Engineering, 46(6), pp. 1559-1575.
https://doi.org/10.1007/s00603-013-0382-y

[4] Yu T, Bastawros AF, Chandra A (2017) Experimental and modeling characterization of wear and life expectancy of electroplated CBN grinding wheels. International Journal of Machine Tools and Manufacture, 121pp. 70-80.
https://doi.org/10.1016/j.ijmachtools.2017.04.013

[5] Dai C, Ding W, Xu J (2017) Influence of grain wear on material removal behavior during grinding nickel-based superalloy with a single diamond grain. International Journal of Machine Tools and Manufacture, 113pp. 49-58. https://doi.org/10.1016/j.ijmachtools.2016.12.001

[6] Li B, Yin J, Zhu Y (2020) Grain wear evolution of cubic boron nitride abrasives during single grain grinding of powder metallurgy superalloy FGH96. Ceramics International.
https://doi.org/10.1016/j.ceramint.2020.09.094

[7] Sieniawski J, Nadolny K (2018) Experimental study into the grinding force in surface grinding of steel CrV12 utilizing a zonal centrifugal coolant provision system. Proceedings of the Institution of Mechanical Engineers, Part B: Journal of Engineering Manufacture, 232(3), pp. 394-403.
https://doi.org/10.1177/0954405416645256

[8] Li Z, Ding WF, Ma CY (2017) Grinding temperature and wheel wear of porous metal-bonded cubic boron nitride superabrasive wheels in high-efficiency deep grinding. Proceedings of the Institution of Mechanical Engineers, Part B: Journal of Engineering Manufacture, 231(11), pp. 1961-1971.
https://doi.org/10.1177/0954405415617928

[9] Curtis D, Krain H, Winder A (2021) Impact of grinding wheel specification on surface integrity and residual stress when grinding Inconel 718. Proceedings of the Institution of Mechanical Engineers, Part B: Journal of Engineering Manufacture, 235(10), pp. 1668-1681.
https://doi.org/10.1177/0954405420961209

[10] Li Q, Xiu S, Yao Y (2020) Study on surface material removal uniformity in double side grinding based on grain trajectories. The International Journal of Advanced Manufacturing Technology, 107(3), pp. 2865-2873.
https://doi.org/10.1007/s00170-020-05147-7

[11] Qu C, Lv Y, Yang Z (2019) An improved chip-thickness model for surface roughness prediction in robotic belt grinding considering the elastic state at contact wheel-workpiece interface. The International Journal of Advanced Manufacturing Technology, 104(5-8), pp. 3209-3217.
https://doi.org/10.1007/s00170-019-04332-7

[12] Hsu SM, Shen MC, Ruff AW (1997) Wear prediction for metals. Tribology International, 30(5), pp. 377-383.

https://doi.org/10.1016/S0301-679X(96)00067-9
[13] Zhang GL and Liu Y and Wang YC (2019) A friction-dissipation based method for quantity model and prediction of graphite/WC-Ni wear under dry sliding. *Tribology* 39(2): 221-227.
10.16078/j.tribology.2018109.
[14] Ma JM, Chen J, Li J (2015) Wear analysis of swash plate/slipper pair of axis piston hydraulic pump. Tribology International, 90pp. 467-472.
https://doi.org/10.1016/j.triboint.2015.05.010
[15] Ramalho A (2015) Wear modelling in rail–wheel contact. Wear, 330-331pp. 524-532.
https://doi.org/10.1016/j.wear.2015.01.067
[16] Gao B, Bao W, Jin T (2021) Variation of wheel-work contact geometry and temperature responses: Thermal modeling of cup wheel grinding. International Journal of Mechanical Sciences, 196
https://doi.org/10.1016/j.ijmecsci.2021.106305
[17] Wang W, Salvatore F, Rech J (2018) Comprehensive investigation on mechanisms of dry belt grinding on AISI52100 hardened steel. Tribology International, 121pp. 310-320.
https://doi.org/10.1016/j.triboint.2018.01.019
[18] Archard JF (1953) Contact and Rubbing of Flat Surfaces[J]. J. Appl. Phys, 24(8). 981-988.
https://doi.org/10.1063/1.1721448
[19] Hou ZB, Komanduri R (2003) On the mechanics of the grinding process – Part I. Stochastic nature of the grinding process. International Journal of Machine Tools and Manufacture, 43(15), pp. 1579-1593.
https://doi.org/10.1016/S0890-6955(03)00186-X
[20] Hecker RL, Liang SY, Xiao JW (2007) Grinding force and power modeling based on chip thickness analysis. The International Journal of Advanced Manufacturing Technology, 33(5-6), pp. 449-459.
https://doi.org/10.1007/s00170-006-0473-y
[21] Madopothula U, Lakshmanan V (2017) Prediction of temperature distribution in the workpiece during multi-pass grinding by finite volume method. International Journal of Precision Engineering and Manufacturing 18(11): 1485-1493.
https://doi.org/10.1007/s12541-017-0176-3

[22] Hahn R S (1962) On the nature of the grinding process[C] Proceedings of the 3rd Machine Tool Design and Research Conference. 126-154.
[23] Li BK, Li CH, Zhang YB (2016) Grinding temperature and energy ratio coefficient in MQL grinding of high-temperature nickel-base alloy by using different vegetable oils as base oil. *Chinese Journal of Aeronautics* 29(4):1084-1095.
CNKI:SUN:HKXS.0.2016-04-023
[24] Lee RS and Jou JL (2003) Application of numerical simulation for wear analysis of warm forging die. Journal of Materials Processing Technology, 140(1-3), pp. 43-48.
https://doi.org/10.1016/S0924-0136(03)00723-4
[25] Tao W and Zhong Y and Feng H (2013) Model for wear prediction of roller linear guides. *Wear* 305(1-2): 260-266.
https://doi.org/10.1016/j.wear.2013.01.047
[26] Niżankowski C and Struzikiewicz (2017). Comparative tests of the proper active grinding powers and maximum grinding temperatures, conducted on corrosion-resistant steel surfaces, using aluminium oxynitride and noble electrocorundum grinding wheels. The International Journal of Advanced Manufacturing Technology, 89(1-4), pp. 273-282.
https://doi.org/10.1007/s00170-016-9084-4

Statements & Declarations

Funding The author(s) disclosed receipt of the following financial support for the research, authorship, and/or publication of this article: This work was financially supported by the National Natural Science Foundation of China (No.52175113, No.51905406), the Key Laboratory Research Program of Education Department of Shaanxi Province (No.18JS044) and the International Science and Technology Cooperation and Exchange Program of Shaanxi Province (No.2020KW-014).

Competing Interests The author(s) declared no potential conflicts of interest with respect to the research, authorship, and/or publication of this article.

Author Contributions All authors contributed to the study conception and design. Modeling, simulation and paper writing were carried out by Cao Wei and Han Zhao, experiments and data processing were completed by Chen Ziqi, Jin Zili and Wu Jiajun,

and manuscript materials were sorted out by Qu Jinxiu and Wang Dong. All authors read and approved the final manuscript.